

SANDIA REPORT

SAND98-1951

Unlimited Release

Printed September 1998

Characterization of Commercial Fiber Optic Connectors- Preliminary Report

Larry A. Andrews and Randy J. Williams

Prepared by
Sandia National Laboratories
Albuquerque, New Mexico 87185 and Livermore, California 94550

Sandia is a multiprogram laboratory operated by Sandia Corporation,
a Lockheed Martin Company, for the United States Department of
Energy under Contract DE-AC04-94AL85000.

Approved for public release; further dissemination unlimited.



Sandia National Laboratories

Issued by Sandia National Laboratories, operated for the United States Department of Energy by Sandia Corporation.

NOTICE: This report was prepared as an account of work sponsored by an agency of the United States Government. Neither the United States Government nor any agency thereof, nor any of their employees, nor any of their contractors, subcontractors, or their employees, makes any warranty, express or implied, or assumes any legal liability or responsibility for the accuracy, completeness, or usefulness of any information, apparatus, product, or process disclosed, or represents that its use would not infringe privately owned rights. Reference herein to any specific commercial product, process, or service by trade name, trademark, manufacturer, or otherwise, does not necessarily constitute or imply its endorsement, recommendation, or favoring by the United States Government, any agency thereof, or any of their contractors or subcontractors. The views and opinions expressed herein do not necessarily state or reflect those of the United States Government, any agency thereof, or any of their contractors.

Printed in the United States of America. This report has been reproduced directly from the best available copy.

Available to DOE and DOE contractors from
Office of Scientific and Technical Information
P.O. Box 62
Oak Ridge, TN 37831

Prices available from (615) 576-8401, FTS 626-8401

Available to the public from
National Technical Information Service
U.S. Department of Commerce
5285 Port Royal Rd
Springfield, VA 22161

NTIS price codes
Printed copy: A03
Microfiche copy: A01



Characterization of Commercial Fiber Optic Connectors-Preliminary Report

Larry A. Andrews
Passive Devices/Interconnects Department
Randy J. Williams
Frequency Device Applications Department

Sandia National Laboratories
P. O. Box 5800
Albuquerque, NM 8185-0523

Abstract

Several types of commercial fiber optic connectors were characterized for potential use in a Sandia designed Laser Diode Ignition (LDI) system. The characterization included optical performance while the connectors were subjected to the more dynamic environmental conditions experienced in weapons applications. The environmental testing included temperature cycling, random vibration, and mechanical shock.

This report presents a performance assessment of the fiber optic connectors and fiber included in the characterization. The desirable design features are described for a fiber optic connector that must survive the dynamic environment of weapon systems. The more detailed performance of each connector type will be included as resources permit.

Funding for this project was discontinued prior to completion of the characterization and documentation of the work. Motivation to document the available information came from the numerous inquiries, both internal and external.

This page intentionally left blank.

Contents

ABSTRACT	3
INTRODUCTION.....	6
BASIC FIBER OPTIC CABLE CONSTRUCTION	7
CONSIDERATIONS FOR FIBER SELECTION	7
BASIC FIBER OPTIC CONNECTOR CONSTRUCTION.....	10
CONNECTOR LOSS MECHANISMS	11
PHASE 1 HARDWARE	12
PHASE 1 TEST SEQUENCE.....	13
EXPERIMENTAL ARRANGEMENT.....	14
RESULTS OF PHASE 1 CHARACTERIZATION.....	15
RESULTS OF PHASE 2 CHARACTERIZATION.....	17
FIBER TESTING	17
CONCLUSIONS	18
REFERENCES.....	19

Figures

FIGURE 1. FIBER OPTIC CABLE CONSTRUCTION	7
FIGURE 2. NUMERICAL APERTURE OF OPTICAL FIBER.....	8
FIGURE 3. FIBER OPTIC CONNECTORS	10
FIGURE 4. CONNECTOR TEST AXES	14
FIGURE 5. EXPERIMENTAL ARRANGEMENT	15
FIGURE 6. OPTICAL THROUGHPUT OF ST CONNECTOR (CERAMIC FERRULE) DURING MECHANICAL SHOCK EVENT	16
FIGURE 7. OPTICAL THROUGHPUT OF SMA CONNECTOR (STAINLESS STEEL FERRULE) DURING MECHANICAL SHOCK EVENT	16
FIGURE 8. OPTICAL FIBER ATTENUATION AS A FUNCTION OF TEMPERATURE.....	18

Tables

TABLE 1. TYPICAL FIBER OPTIC CABLE MATERIALS.....	9
TABLE 2. CONNECTOR TEST MATRIX.....	14

Introduction

Fiber optic subsystems offer advantages over traditional electrical approaches in some applications. One application being developed by Sandia National Laboratories is the Laser Diode Ignition (LDI) subsystem that would use optical energy to ignite energetic components (actuators, initiators, and detonators). In this subsystem, an optical fiber couples the output of a laser diode to the energetic component. The explosive component itself is immune to electrical interference and optical coupling makes the entire subsystem less sensitive to unintended electrical signals, a desirable safety attribute.

Generally, commercially available fiber optic connectors are designed for the relatively benign telecommunications environments and performance characteristics in the dynamic environments (extreme temperature cycling, vibration, and mechanical shock) experienced in weapons applications are not defined. As part of the LDI program, a fiber optic characterization project was implemented to identify the connector design and fiber type most suitable for weapon applications. The LDI program drove fiber optic performance requirements. The program required an optical cable assembly that would maintain the ability to pass sufficient optical energy from a pulsed laser diode during and after typical weapons environments (random vibration, mechanical shock, and temperature cycling). The testing was originally defined to consist of three phases. Phase 1 would characterize various designs of fiber optic connectors to identify the “best” type for our applications. The hardware selected for evaluation in the Phase 1 testing included the SMA 906 with stainless steel ferrule, SMA 906 with ceramic (Al_2O_3) ferrule, ST with stainless steel ferrule, ST with ceramic (Al_2O_3) ferrule, NTT FC/PC with stainless steel ferrule, and Mini-BNC with stainless steel ferrule. A late addition to the test was the Radiall MILFO Optiball connector with a stainless steel ferrule. All cable assemblies were fabricated with the same type of optical fiber cable.

The second phase was to be a thorough evaluation of the selected connector type (i.e., the type that performed best during the Phase 1 testing). The evaluation was to include samples representing the various design interpretations and materials of the selected connector type from different connector manufacturers. Potential design modifications to a given design would also be evaluated at this time. The Phase 2 testing was to include mechanical shock and random vibration at the temperature extremes.

The final phase of the characterization project would be a detailed investigation of multimode optical fibers from different suppliers using the best connector design. The evaluation would consider cable construction and fabrication techniques (epoxy, fiber polishing, etc.) most suitable for our applications.

Although program funding was canceled before Phases 2 and 3 could be adequately addressed, some of the more critical issues were investigated to some degree. With the cancellation of funding came the lack of formal documentation of the results from the testing that was completed. This summary is a preliminary report of the work completed prior to cancellation. Absent is the detailed performance information of each connector type for any given test.

Basic Fiber Optic Cable Construction

As a minimum, a fiber cable will consist of a core, cladding, strength member, and jacket. To maintain total internal reflection, the refractive index of the cladding is less than the refractive index of the core. Some cable designs may include a coating and/or buffer over the fiber to extend the environmental performance range. The basic construction is shown in Figure 1. Additional information on materials for each of these cable attributes is provided in the next section.

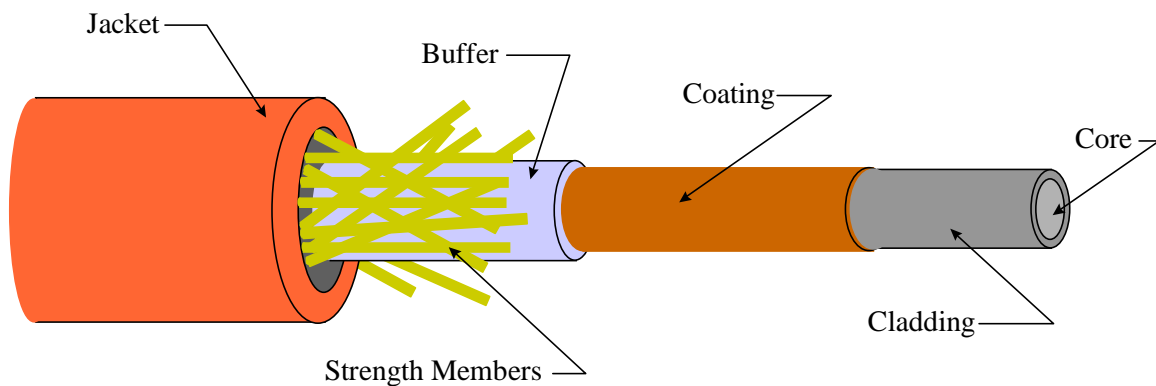


Figure 1. Fiber Optic Cable Construction

Considerations for Fiber Selection

In selecting a fiber for a given application, there are several issues to consider. Fiber characteristics and materials and cable jacket materials are selected to optimize performance in a particular application. Fiber characteristics to consider may include the numerical aperture (NA), core diameter, multimode or single mode, attenuation at operating wavelength, minimum bend radius and radiation resistance. Environmental considerations such as operating temperature range, mechanical shock, vibration, and crush resistance will also influence the selection of buffer and cable jacket materials.

For power transmission applications, such as LDI, there are trade offs to consider in coupling efficiency and output power density. Coupling efficiency

decreases as source divergence and fiber-to-source separation increases. A large core diameter fiber with a high numerical aperture (NA) will gather more light from the source. Figure 2 illustrates the definition of numerical aperture.

At the output end of the fiber, smaller core diameter and smaller NA (less divergent output) are desirable if power density is important. Power density is inversely proportional to the square of the fiber core radius.

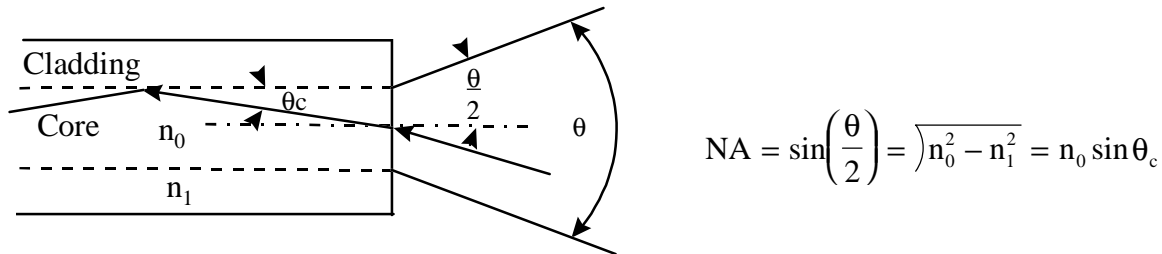


Figure 2. Numerical Aperture of Optical Fiber

For LDI, a fairly large core diameter is needed to optimize coupling efficiency between the laser diode source and the fiber while maintaining moderate power density at the energetic component. It is basically a given that multi-mode fiber is required (single mode fiber core diameters are on the order of $7\mu\text{m}$ while multi-mode fiber cores are $\geq 50\mu\text{m}$ in diameter).

Ionizing radiation will also influence the optical performance of fiber. Low OH fibers will darken (permanent increase in attenuation) at a lower total dose than the high OH fibers. The increase in attenuation can be attributed to light leakage (from a change in the index of refraction of the core and cladding, for example), or light absorption by color centers [1]. High OH, glass-on-glass fibers have demonstrated superior performance in ionizing radiation environments but at the expense of higher intrinsic attenuation, (14dB/km @ 820nm). A study by Lyons, et. al., concluded that polyimide coated fibers (silica core, fluorosilica cladding) outperformed acrylate coated fibers during exposure to a Co^{60} source. There was no significant difference in the performance of fibers with either coating during exposure to transient radiation [2].

The strength of the bare fiber is greatly influenced by the presence of flaws. Under stress, such as a bend, propagation of the crack can result in a complete fracture of the fiber (static fatigue). The time to failure can be accelerated if the fiber is exposed to moisture. Some types of fiber coatings, such as polyimide and carbon, can improve static fatigue performance by slowing or preventing moisture from accumulating in surface flaws [3]. (That is, the mean time to failure can be increased for a given bend radius and fiber diameter.)

Unfortunately, some of the same coatings that improve static fatigue performance can degrade low temperature performance [4].

The fiber cable is designed to protect the fiber in its use environment. The material selected for each component of the cable is intended to mitigate a particular environmental or mechanical threat. As a minimum, the fiber cable will require a strength member to carry the longitudinal load and an outer jacket to provide some moisture and abrasion resistance. Cables may be designed with buffers to increase crush resistance and reduce susceptibility to mechanically or thermally induced microbends by providing additional mechanical decoupling between the fiber and outer jacket. (Microbends can be introduced into the fiber from distortions in the outer jacket, either due to an external mechanical load or as a result of the differences in the coefficient of thermal expansion (CTE) between the jacket and fiber. The resilient buffer minimizes the interaction between the jacket and fiber.)

For proper cable design, one should consider the mechanical environment (vibration, shock, flexing, crush, bend radius, etc.), temperature, and humidity requirements. A list of some typical cable materials and capabilities is included as a reference in Table 1. This table is not presented as an exhaustive list, but only as an example of cable materials.

Table 1. Typical Fiber Optic Cable Materials

Core	Cladding	Coating	Buffer	Strength Members	Jacket (Inner &/or outer)
Silica (pure or doped, e.g. Ge or F)	Silica (pure or doped)	Polyimide (up to 375°C)	Acrylate (up to 80°C)	Kevlar (Aramid Yarn)	Polyurethane-55 to 100°C 570 lbs crush
Plastic	Plastic	"Polymer Hardcoat"	Silicone	Steel	Polyethylene (-60 to 80°C)
	"Polymer Hardcoat" (a proprietary material of some suppliers)	Gold	Tefzel	Glass/Epoxy	PVC (-20 to 80°C)
		Carbon			Hytrel
					Tefzel (Fluorocopolymer thermoplastic, -65 to 150°C) 285 lbs crush

Basic Fiber Optic Connector Construction

Two basic concepts of fiber optic connector design were evaluated. A non-contacting type (represented by the SMA type and the Radiall MILFO) and the face contact (represented by the ST, NTT FC/PC, and the Mini-BNC). The non-contacting ferrule type is designed for an inherent gap (set by the length of the ferrule and controlled with the polishing tool) between properly terminated mated pairs. The disadvantage of this design is the higher insertion loss introduced by the gap between fiber ends. Manufacturers' data shows average insertion loss approaching 1dB.

In the contacting type designs (face contact and point contact), the polished fiber ends of a mated connector pair are forced into contact by spring loaded ferrules. The ferrule ends (in the plane parallel to the fiber face) are designed with a large radius to ensure fiber-to-fiber contact of properly terminated connectors, minimizing losses due to Fresnel reflection and end separation. This type of connector design offers lower insertion loss (manufacturer's specifications typically claim <0.5dB). The general difference between the non-contacting and contacting is illustrated in Figure 3. The figure also illustrates two typical approaches to the coupling ring. Several designs incorporate a threaded coupling ring (SMA, NTT FC/PC, and Radiall MILFO). The ST and Mini-BNC use bayonet pins (similar to the BNC electrical connector).

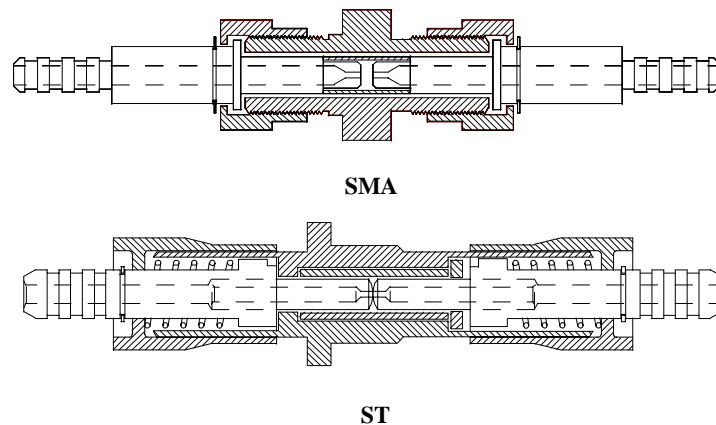


Figure 3. Fiber Optic Connectors

Angular and lateral alignment is accomplished with alignment sleeves that are typically part of the coupler. Common alignment sleeve materials are beryllium copper (BeCu) and zirconia ceramic. The inside diameter of the alignment sleeve is slightly smaller than the ferrule outside diameter. A split along the length of one side allows the sleeve to spring open and maintain a tight fit as the ferrule is

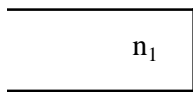
inserted into the coupler. Notable variations in alignment sleeves are the SMA 906 and the Radiall MILFO. The SMA connectors use a plastic sleeve that is a press fit over the necked down portion of the ferrule. The Radiall uses a more complex arrangement that can be roughly described as a circumferential V-groove on the shoulder of the ferrule. Alignment is accomplished as the reduced diameter ferrule tip enters the through hole of the alignment ball and the edge of the hole aligns with the ferrule v-groove. Cross sections of the various designs will be included in the final report.

Typical connector materials for the connector body and couplers included brass and die-cast zinc for the connector body and couplers. Ferrule materials typically included stainless steel or alumina (Al₂O₃).

Connector Loss Mechanisms

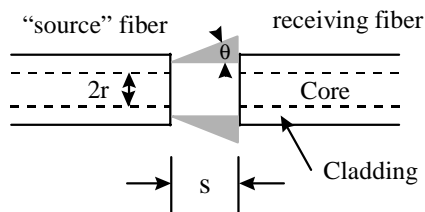
There are several types of losses that can occur when coupling fibers. Some of the more typical are illustrated below. Proper design of the fiber optic connector and coupler attempts to minimize the effect of each condition. For example, connector designs using physical contact ferrules minimize Fresnel reflection and end separation losses. Alignment sleeves minimize angular and lateral misalignment losses. The illustrated conditions are for fibers with matching core areas and numerical aperture. Additional losses will occur if the NA of the receiving fiber is less than the NA of the transmitting fiber ($10\log[NA_R/NA_T]^2$) or if the core diameter of the receiving fiber is less than that of the transmitting fiber ($10\log(r_R^2/r_T^2)$).

1. Fresnel reflection losses are due to a mismatch in the indices of refraction.



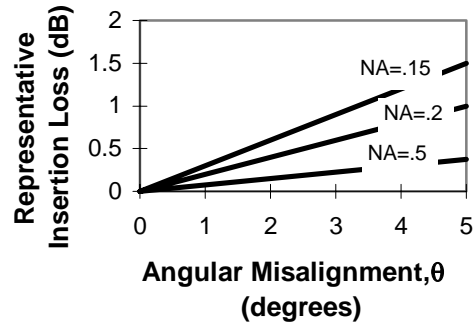
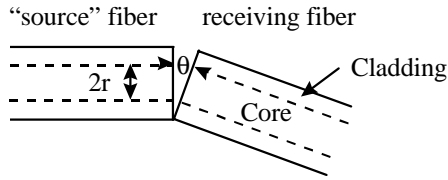
$$R = \left[\frac{n_1 - n_0}{n_1 + n_0} \right]^2$$

2. End Separation

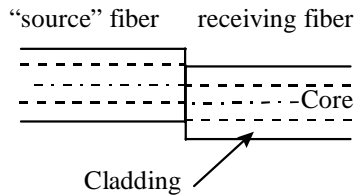


$$\text{Loss} = 10\log \left[\frac{r}{r + (s * \tan(\sin^{-1}(NA/n_0)))} \right]$$

3. Angular Misalignment



4. Lateral Misalignment



Phase 1 Hardware

Eight mated pairs of each type were included in the evaluation. All test samples were prepared by attaching the connector under test to one end of a 10m long fiber cable. The opposite end of all cable assemblies was terminated with ST connectors to maintain interface compatibility with our test equipment. All cables were fabricated with Ensign-Bickford HCG-M0100T-C01US-14. This is a 0.22 NA Step Index multi-mode high-OH fiber. The core is 100 μ m diameter pure fused silica with a 130 μ m diameter doped silica cladding and a proprietary hard polymer coating for an overall diameter of 140 μ m. Over the fiber are a Tefzel buffer, Kevlar strength member and a polyurethane outer jacket. The fiber provided the desired optical properties for the LDI application. Since the testing was going to consume over a kilometer of cable, the lower cost offered by the polyurethane jacket was selected. The third phase of the characterization was to take a closer look at an "aerospace" cable design that adds an inner jacket of Hytrel over a silicone buffer and incorporates a Tefzel outer jacket in place of the polyurethane. All fiber terminations were made using EPO-TEK 353ND epoxy. Cable terminations and fiber polishing were in accordance to manufacturers' instructions for each connector type.

Phase 1 Test Sequence

The general test sequence and test descriptions are given below. The test matrix in Table 2 shows the quantity of connectors subjected to each test.

1. **Visual Inspection.** Initial inspection: cables with cracks or chips in the core of the polished fiber face were unacceptable and the cables were reworked. Minor cracks in outer diameter of cladding were considered acceptable and documented accordingly.
2. **Insertion Loss (Relative to a Reference Cable).** The optical power transmitted through the cable was measured using a laser diode source and PIN diode detector. Any cables with a transmission efficiency of less than 90% of the established reference cable were reworked.
3. **Temperature Cycle.** Mated pairs of the connectors under test were subjected to 10 thermal cycles. Each cycle consisted of one-hour minimum at -55°C and one hour minimum at 100°C . The oven transfer time between temperature extremes was ≤ 5 minutes.
4. **Mechanical Shock I.** Mated test pairs were subjected to a 3500g/0.5ms haversine mechanical shock in the X and Y direction at room temperature. Refer to Figure 4 for definition of axes.
5. **Random Vibration I.** Mated connector test pairs were subjected to random vibration of 9 grms over the frequency range of 10 to 2000 Hz for 20 minutes in each the X and Y axis. Refer to Figure 4 for definition of axes.
6. **Random Vibration II.** Mated connector test pairs were subjected to random vibration of 16 grms (raised to 24 grms after one uneventful test at 16 grms) over the frequency range of 10 to 2000 Hz for 10 minutes in each the X and Y axis. Refer to Figure 4 for definition of axes.
7. **Long Term Vibration.** Mated connector test pairs were subjected to random vibration of 16 grms over the frequency range of 10 to 2000 Hz for 7.5 hours in each the X and Y axis for a total vibration time of 15 hours. Refer to Figure 4 for definition of axes.
8. **Final inspection.** Note any cracking, breaking, loosening, or other damage that might affect fit or function.

Fixturing for the mechanical shock and random vibration testing was accomplished by securing the threaded coupler into a .125" thick test plate with a jam nut. The test plates were then attached to the shock/vibration fixture leaving only the area immediately around the coupler unsupported.

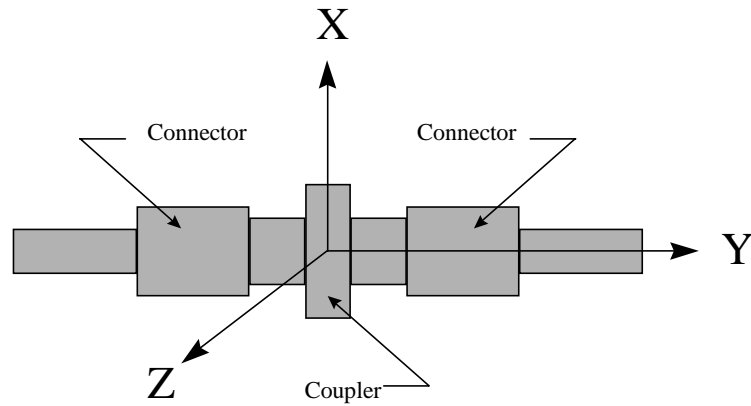


Figure 4. Connector Test Axes

Table 2. Connector Test Matrix

Connector Type	Temperature Cycle (-55 to 100 C)	Mech. Shock 3500g, 0.5ms	Random Vibration			
			9 grms, 20 min./axis	16 grms, 10 min./axis	24 grms, 10 min./axis	16 grms, 7.5 hr./axis
ST, ss	8	8	8	2 *	2	4
ST, ceramic	8	4 **	4	--	4	4
Mini-BNC, ss	8	8	8	--	--	--
SMA906, ss	8	8	8	--	4	4
SMA906, ceramic	8	8	8	--	4	4
NTT FC/PC, ss	--	8	8	--	--	--
Radial MILFO, ss	--	8	--	--	--	7

* Random vibration level increased to 24 grms after uneventful test at 16 grms.

** After all four mated pairs of ST connectors with ceramic ferrules failed during the first mechanical shock, the second connector set was not subjected to the mechanical shock so that samples would be available for the vibration test.

Experimental Arrangement

A five-way splitter was coupled to the output of a laser diode. Four branches were used to power four mated pairs under test. The fifth fiber branch was used to monitor source stability and was not subjected to the test environment. Optical throughput of each branch was monitored with an FND100 PIN diode. The arrangement is represented schematically in Figure 5.

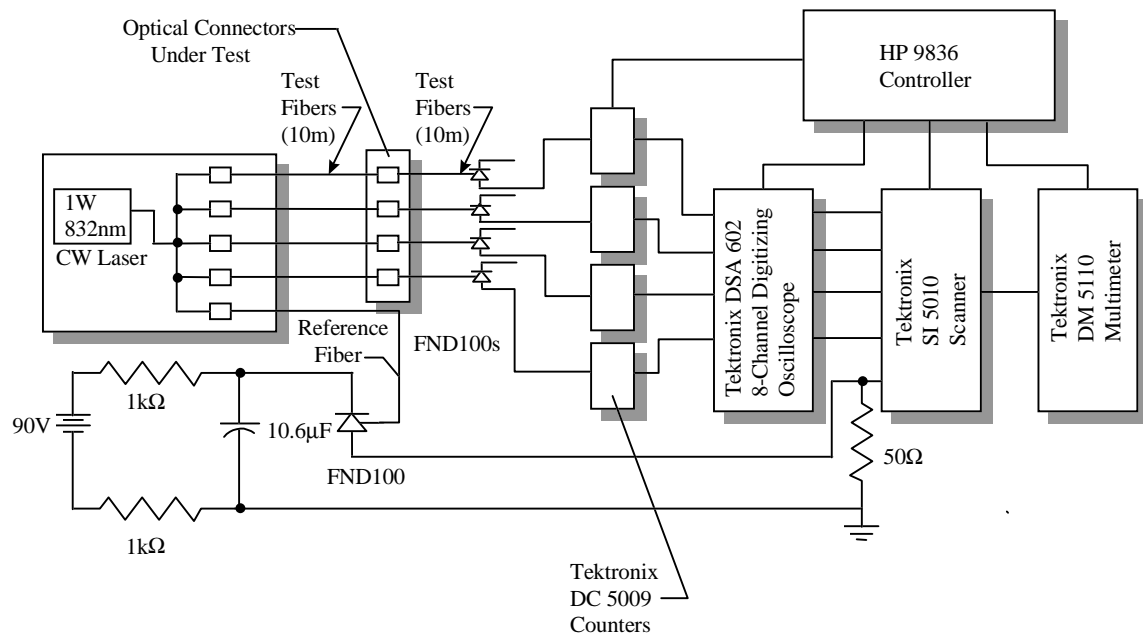


Figure 5. Experimental Arrangement

Results of Phase 1 Characterization

All connectors using the spring-loaded, face-contact ferrule design experienced transient disconnects in the mechanical shock environments. Shocks in the Y-direction (along the axis of the ferrule) caused a more significant interruption of the optical signal during and up to 1ms after the shock event. The recovery time could be caused by “chatter” as the springs force the ferrules back into contact. The transient losses are dominated by end separation losses. Transient losses during the X/Z direction losses can be attributed to angular and lateral misalignment. The ceramic-ferrule ST connectors were vulnerable to breaking during shocks in the X/Z direction (fracture of the fiber resulting in permanent loss of the optical signal) as demonstrated with five out of eight ferrules breaking during shocks of 3500gs. Figure 6 illustrates the typical response of the ceramic-ferrule ST connector in the mechanical shock environment. The ceramic ferrules of the ST connectors may have been more susceptible to fracturing due to its longer unsupported length in comparison to the SMA. Failure of mechanical locking features (bayonet pins, etc.) would result in a permanent increase in attenuation. The bayonet pins of three Mini-BNC connectors broke during mechanical shock.

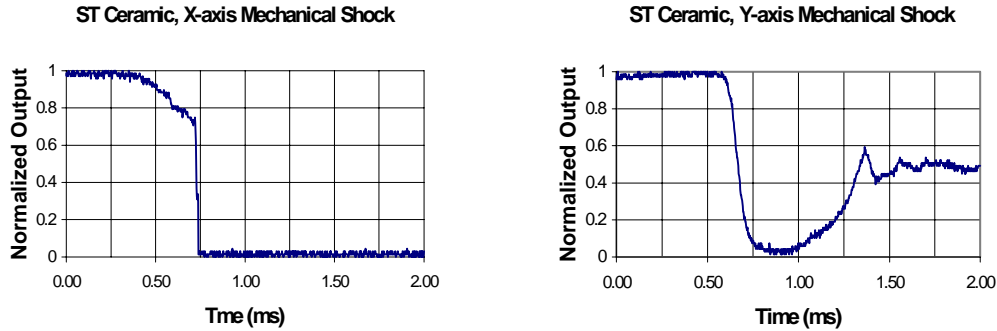


Figure 6. Optical Throughput of ST Connector (Ceramic Ferrule) During Mechanical Shock Event

The SMA and MILFO connectors proved to be adequate (period of increased attenuation is short compared to the 10ms laser pulse of the LDI system) in shock environments of any direction. Both of these connector types are designed for an inherent gap of .001”- .002” between mated ferrule ends and neither uses spring-loaded ferrules. Transient losses in the non-spring loaded ferrule connectors may be attributed to angular and lateral misalignment. Figure 7 illustrates the typical response of the stainless steel ferrule SMA connector in the mechanical shock environment.

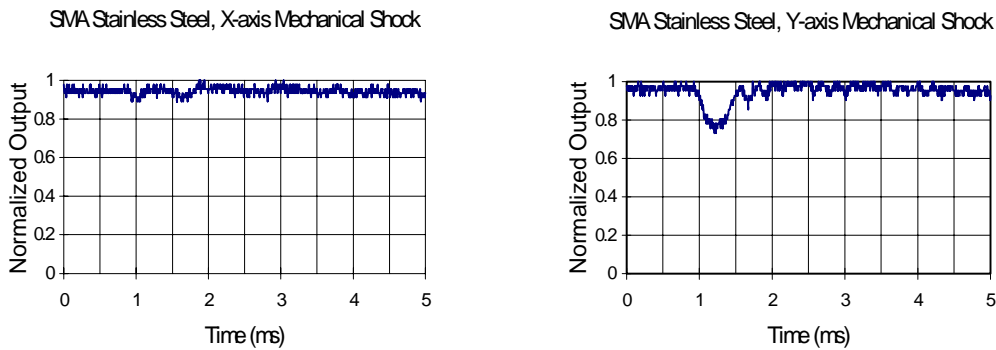


Figure 7. Optical Throughput of SMA Connector (Stainless Steel Ferrule) During Mechanical Shock Event

All designs performed well through random vibration. The suspected vulnerability of the contacting ferrules (all designs but the SMA and MILFO) abrading the fiber/ferrule ends (thus increasing insertion loss by physical damage or debris) did not occur during vibration.

The insertion loss that was observed during thermal cycling was demonstrated to be a phenomenon of fibers with coating (e.g., polyimide and hard polymer coatings). The fiber testing is discussed in a later section.

The Phase 1 testing identified several desirable design features for a fiber optic connector required to function in dynamic environments. These features include a threaded coupling nut, non-spring loaded and non-contacting ferrule. An environmentally sealed optical interface and a keyed mating interface (to prevent ferrule rotation and provide a repeatable insertion loss with a given mated pair) also added to the list of desirable features. The Mil-C-83522 version of the SMA includes an o-ring seal and meets all of these requirements except for the keyed interface. Towards the end of the Phase 1 testing the Radial MILFO also “discovered”, which appeared to meet all of our design criteria and samples were purchased for our abbreviated Phase 2 testing.

Results of Phase 2 Characterization

Sixteen cable assemblies were fabricated with Radial MILFO connectors providing eight mated connector pairs testing. Because of the limited time prior to expiration of program funding, the testing was prioritized, selecting the mechanical shock and long term random vibration tests as the most demanding. The results of these tests indicated that the Radial MILFO was capable of performing in our environments. The ferrule alignment feature in the coupler also appeared to be superior to the SMA.

Fiber Testing

The losses observed during the thermal cycling appeared to track the temperature cycle (attenuation increased during the low temperature exposure), regardless of the connector type. The fiber was the suspected cause and literature research suggested that the losses might be due to microbending losses resulting from the mismatch in CTE between the cladding and any tightly adhering fiber coating (e.g., polyimide, hard polymer coatings, etc.) [4]. An unfortunate side effect given the improved static fatigue performance provided by these coatings. Similar losses can also occur in uncoated fibers due to a CTE mismatch between the fiber and outer jacket. In this case, the losses may be minimized by including a resilient buffer material (e.g., silicone) over the fiber.

Additional temperature cycling tests were conducted with continuous loops of fiber in the temperature chamber (all connections were made outside of the chamber). The testing compared the performance of three fibers with coating bonded directly to the cladding and one uncoated fiber with a “loose” acrylate buffer. The fibers with coating were 1) 400/440 fiber (core diameter in μm /cladding diameter in μm) with a 15 μm polyimide coating, 2) 100/140 fiber with a 15 μm polyimide coating, 3) 100/130 fiber with a 5 μm hard polymer coating (the fiber used in all previous connector testing described in this report), and 4) 100/140 fiber with an acrylate buffer. The samples were arranged so that 26 feet of fiber, in a 10-inch diameter coil, were in the temperature chamber.

The fiber with the “loose” acrylate buffer was largely immune to the thermal cycling. The samples with coatings suffered an increase in attenuation below 0°C with polyimide coating on the small diameter fiber being the poorest performer. The 400/440 fiber with polyimide coating performed better than the 100/140 polyimide coated fiber, possibly due in part to the greater stiffness (resistance to microbending) of the larger diameter fiber. As a comparison, the normalized output versus temperature is shown in the graph of Figure 8.

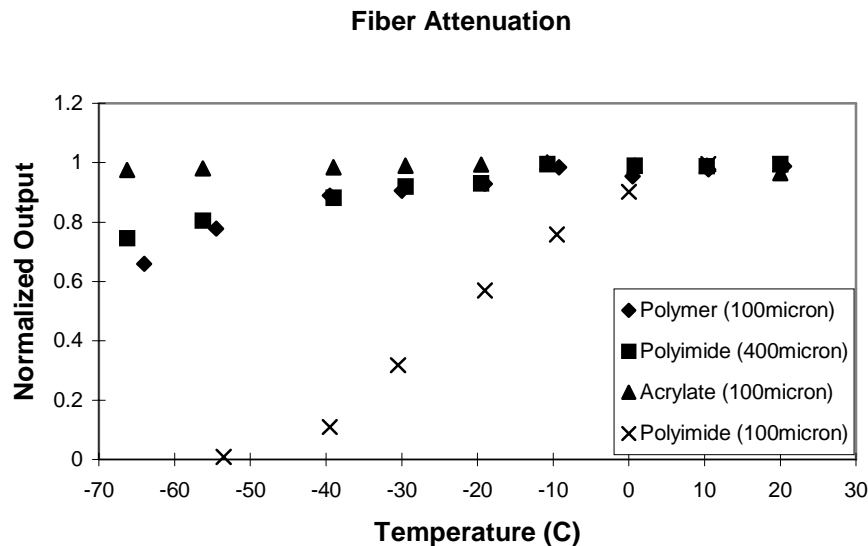


Figure 8. Optical Fiber Attenuation as a Function of Temperature (Polyimide data are an average of four samples. The polymer and acrylate data are an average of two samples each.)

Conclusions

The face contacting (spring loaded ferrule) design offered lower initial insertion loss. In addition to the contacting ferrules, precision ceramic ferrules help to reduce insertion loss. However, these designs proved vulnerable to mechanical

shock environments. Shocks in the Y-direction (along the axis of the ferrule) could cause a complete loss of signal during the 3500g/0.5ms pulse and for up to 1ms following the shock pulse. Mechanical shocks in the X-direction (perpendicular to the ferrule) resulted in broken ceramic ferrules in five of the eight ST connectors. The shorter ceramic ferrule of the SMA 906s survived our mechanical shock levels. All connectors performed surprisingly well during random vibration of up to 15 hours at 16 grms. Insertion loss during temperature cycling was dominated by the performance of fibers (suspected microbending losses due to the mismatch in expansion between the fiber and coatings)

The Phase 1 testing identified several desirable features for a fiber optic connector that is to be used in a weapons environment. These features include a threaded coupling nut, environmentally sealed optical interface, keyed mating interface, non-spring loaded ferrule, and non-contacting ferrules.

Our original recommendation for the baseline design in the LDI application was the SMA 906 fiber optic connector. Interestingly, it was the oldest and least expensive design of the connectors evaluated. Had the program continued, both the Mil-C 83522 version of the SMA 906 (stainless steel ferrule with o-ring seal) and the Radiall MILFO would have been evaluated through a complete environmental sequence (i.e., mechanical shock and random vibration at temperature extremes).

Although the Radiall MILFO was about twice the cost of the SMA (\$25 in 1993 dollars), it performed very well and was a strong contender for the baseline design for the Sandia LDI system.

References

1. R. Toossi and D. Modarress, Radiation and Temperature Survivability of Multimode Step-Index Fluorine-Doped Silica Fibers, IEEE Transactions on Nuclear Science, Vol. 38, No. 5, October 1991.
2. P. Lyons et al., Influence of Preform and Draw Conditions on UV Transmission and Transient Radiation Sensitivity of an Optical Fiber
3. Matthew G. Esteo and G. Scott Glasseman, The effect of carbon on the mechanical behavior of large flaws, SPIE Vol. 1791 Optical Materials Reliability and Testing, 1992.
4. Wing F. Yeung and Alan R. Johnston, Effects of Temperature on Optical Fiber Transmission, Applied Optics, Vol. 17, No, 23, p3703-3705, 1 December 1978.

Distribution

1 0328 D. M. Berry, 2674
1 0328 C. F. Briner, 2674
1 0328 S. C. Holswade, 2674
1 0328 L. S. Weichman, 2674
1 0481 M. A. Rosenthal, 2167
1 0481 M. M. Harcourt, 2167
1 0481 J. M. Montoya, 2167
1 0481 T. M. Skaggs, 2167
1 0481 D. L. Thomas, 2167
1 0481 V. O. Willan, 2167
1 0481 K. D. Meeks, 2168
10 0523 L. A. Andrews, 1733
1 0523 J. O. Harris, 1733
1 0523 T. L. Ernest, 1733
1 0523 J. T. Hanlon, 17331
1 0523 R. D. Kilgo, 1733
1 0525 T. A. Fischer, 1732
10 0525 R. J. Williams, 1732
1 0527 E. P. Royer, 1731
1 0527 S. S. Lopez, 1731
1 0527 F. H. Sieradzki, 1731
1 0549 L. Hinkle, 5932
1 0637 D. F. Davis, 12336
1 1421 R. E. Setchell, 1152
1 1423 R. L. Schmitt, 1128
10 1452 J. A. Merson, 1552
1 1452 F. J. Salas, 1552
1 9013 R. G. Miller, 2266
1 9013 R. D. Sauls, 2266
1 9013 E. Talbot, 2266
1 9036 M. C. Hinckley, 2254
1 9101 R. E. Clark, 8411
1 9102 A. L. Hull, 8416
1 9018 Central Technical Files, 8940-2
2 0899 Technical Library, 4916
2 0619 Review & Approval Desk, 12690
For DOE/OSTI

9 AlliedSignal, FM&T
2000 East 95th Street
Kansas City, MO 64131
2D36 P. Klingsporn, D/ME1-3
2D36 J. Burden, D/ME1-3
2B37 J. M. Emmons, EE7
2B37 D. Lemon, EE7

2B37 R. Schaldecker, EE7
2D39 E. Belarde, EE3
2D39 R. Morris, EE3
MC47 B. O. Hower, ME11
MY40 S. Sunvold, EB33